ELSEVIER

Journal of Power Sources 91 (2000) 51–61

JOURNAL OF POWER SOURCES

www.elsevier.com/locate/jpowsour

Lead acid battery with thin metal film (TMF®) technology for high power applications

Ramesh C. Bhardwaj *, John Than

BOLDER Technologies Corporation, 4403 Table Mountain Drive, Golden, CO 80403, USA

Received 28 May 1999

Abstract

The lead acid battery chemistry has been utilized to support the energy needs of cars and engines starting for the past 100 years. Conventional lead acid batteries are rather large and heavy to meet the power requirements for most applications. BOLDER Technologies Corporation has taken the electrochemical concept of the lead acid battery and made a spirally wound valve regulated lead acid battery based on its patented Thin Metal Film (TMF®) technology. This has small size but more power than any other existing battery. This paper describes the power of the TMF lead acid battery and its applications.

Keywords: Lead acid; High power; HEV; Engine start; TMF; VRLA

1. Introduction

The current collector used in most lead acid batteries is a thick grid of lead or its alloys with Sn, Ca, and/or antimony. These grids are coated with positive or negative paste materials of lead oxide, red lead or lead oxide. The single cell of most lead acid batteries has a single tab terminal for the negative and positive electrodes on top of the cell. The tabs of six single cells are connected with a positive and negative cast-on terminal to make a 12 V battery. These batteries become very heavy for applications where high power is required, due to the inefficient design. The thin metal film technology developed by BOLDER Technology Corporation has combined the knowledge of well established lead acid battery electrochemistry with a novel cell design which is capable of delivering very high power in a very small package and with substantial weight reduction.

The key design aspect of the BOLDER battery is the use of a thin metal film current collector (which provides a very high surface area current collector) instead of a grid, small inter-plate spacing (low impedance) and a continuous foil contact cast-on current carrier in the opposite end of the cell.

This innovative design results in a spirally wound rechargeable valve regulated lead acid battery capable of delivering and accepting extremely high power levels not delivered by any other lead acid battery or batteries with any other chemistries.

By virtue of the large surface area, the continuous foil contact, the cylindrical design along with the opposite end current collector, and the small inter-electrode spacing, the voltage distortion load, due to inductive effects, is minimal. These design aspects make the cell capable of delivering very high current discharge (> 1000 A) and ultra-fast recharge with very high efficiency.

2. Design of the TMF cell

TMF battery technology [1–4] has been developed at BOLDER Technologies Corporation, Golden, CO. The concept represents a unique extrapolation of conventional lead acid technology into a new non-conventional, configuration. The original developers of the sealed lead acid gas-recombinant battery technology used thick perforated electrodes and single point current collection [5]. These two physical aspects introduced inefficiency to the operation of the cell. The construction of TMF batteries consists of a thin (0.003 in.) layer of active paste applied to both sides of a solid (0.003 in.) lead foil. The total thickness of the electrode is thus 0.009 in. or approximately 0.25 mm.

* Corresponding author. Present address: Concorde Battery Corporation, 2009 San Bernardino Road, West Covina, CA 91790, USA. Tel.: +1-626-813-1234, ext. 258.

0378-7753/00/$ - see front matter
PII: S0378-7753(00)00486-9

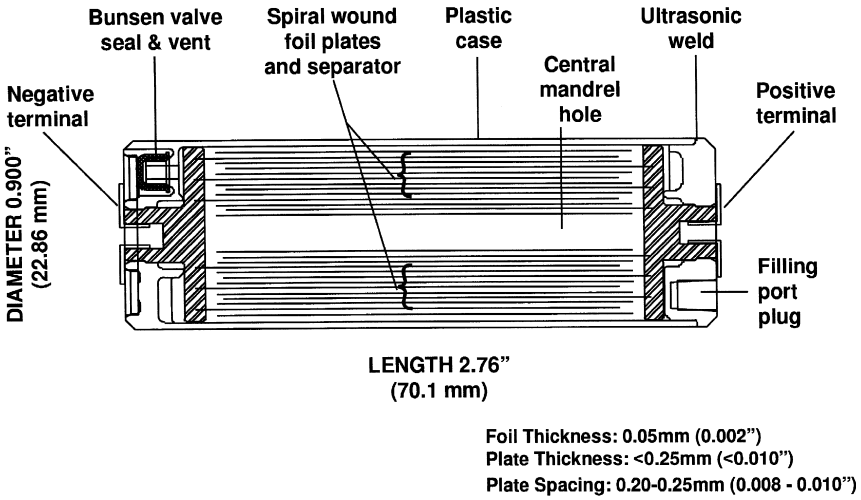

Fig. 1. Cross-section of 1 Ah/2 V sub-C cell.

The precise pasting operation leaves a thin strip of un-coated foil along one edge . The un-coated area forms the contact to the cell terminal. When compared to conventional flooded and sealed lead acid batteries, this design produces a 16–19 times increase in the ratio of plate surface area to active material, and a 20–80 times decrease in the path length of the electron flow. The basic cell design is illustrated in Fig. 1.

The positive and negative elements are wound together in a spiral wrap configuration with a thin (0.008 in.) glass fiber separator. The cell is wound in a manner to permit the un-coated strip on the lead foil collector of each element to protrude slightly from the end of the wound cell. Thus, un-coated areas of each plate polarity protrude from opposite ends of the wound cell (similar to capacitor designs). The lead terminals are cast onto the full length of the exposed ends of the spirally wrapped cell. The castings serve as a seal, current collector and manifold for electrolyte distribution. The cell design incorporates a low pressure, Bunsen vent valve. The cell is formed immediately after filling with electrolyte. Physical and electrical characteristics of the 1.0 Ah/2 V and 5.0 Ah/2 V TMF cell are shown in Table 1.

3. Diffusion model

The diffusion of acid from separator to the active material during discharge determines time of a battery at high current discharges. Fig. 2 shows the comparison of the TMF battery versus a conventional VRLA product in thickness of active material, separator and inter-electrode distance. The paste in the TMF cell is distributed on a high surface area thin film with the thickness of 0.25 mm and the inter-electrode distance is 0.20 mm. This is considerably different to a conventional VRLA battery where the paste thickness is 2 mm and inter-plate spacing varies from 1 to 2 mm. The combination of high surface area with small inter-electrode distance results in low impedance (1.0 mΩ) and extremely fast diffusion of acid from separa-

Table 1
TMF cell specifications for l Ah and 5 Ah

	1 Ah Cell specification	5 Ah Cell specification
Voltage	2.15 V	2.15 V
Capacity	1 Ah @ C rate	5 Ah @ C rate
	0.60 Ah @ 50 C rate for 43 s	3.0 Ah @ 50 C rate for 215 s
Weight (kg)	0.092	0.460
Dimensions		
Diameter (mm)	22.9	49.0
Length (mm)	70.0	82.0
Specific energy (Wh/kg)	28.0	22.0
Energy density (Wh/l)	78.0	67.0
Cell impedance (mΩ)	1.40	0.30
Specific power (W/kg)	4439 (at 270 A)	5329 (1350 A derived)
Instantaneous peak power (W/kg)	4400 (@ 1000 A short circuit	5600 (short circuit across 2 K shunt)
Instantaneous peak power density (W/l)	12,100 (@ 1000 A (short circuit)	16,500 (short circuit across 2 K shunt)

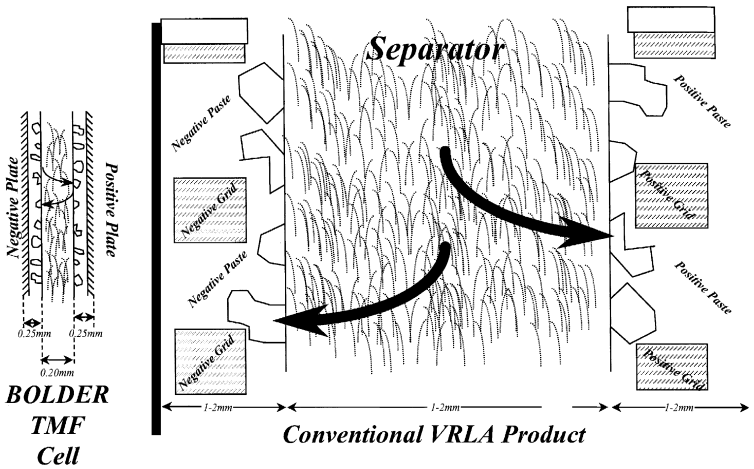

Fig. 2. Diffusion model for conventional VRLA battery and BOLDER TMF cell.

tor to the active material which provides ultra-fast discharge and charge acceptance. The impedance of the cell remains constant even at 70–80% depth of discharge resulting in minimal voltage drop during the discharge. The illustration of impedance versus depth of discharge is shown elsewhere [6–8]. This model therefore provides the rationale for the stiff voltage and the constant power capability of TMF lead acid battery during high rate discharge.

4. General performance of the TMF cell / battery

The first 2 V/1.0 Ah TMF product is spiral-wound single cell, which can be configured easily into 12, 24 or even 300 V batteries and is being commercially produced. It is classified as a 9/5 sub-C product. The second 2 V/5.0 Ah TMF product in the same configuration has also been developed and has been under limited production for beta testing. The power characteristics of both cells are presented in this paper.

The ability to sustain high discharge currents for a lead acid battery is a function of the plate pore structure and the diffusion of electrolyte into the reaction sites. The unique construction of TMF cell with high surface area, close proximity of electrolyte to the plate and continuous foil contact with top lead cast-on terminal contributes to an 'ideal' voltage/time discharge profile that shows a small initial voltage drop from open circuit and a long flat voltage plateau even at 500 A discharge.

The voltage/time curve of a 2.0/1 Ah cell at 1 and 80 A has been reported in earlier papers [9–11]. Fig. 3 shows the voltage/time discharge curves at 300 and 500 A for a BOLDER TMF 2 V/1.0 Ah cell. Table 2 shows the discharge data, calculated specific energy and specific power at constant power as well as constant current.

The voltage/time curve of a 2.0 V/5.0 Ah cell at 40 and 120 A discharge is shown in Fig. 4. Note that there is a minimal voltage separation between the two discharge curves due to the low cell impedance and porous structure available in the active material. Moreover, the voltage plateau is very flat for both curves, indicating that the cells (1 and 5 Ah) are capable of delivering constant power at any C rate up to 500 C. Table 3 shows the constant current discharge data and calculated specific energy and specific power values for the 5 Ah cell.

Specific energy and specific power values are calculated from the data taking into account the cell weights of 82 and 460 g and volumes of 30 and 153 cm^3 for the 1 and 5 Ah cells, respectively.

It is noteworthy that at 500 A discharge, the cells of 1 and 5 Ah delivered 6.5 and ~6.3 Wh/kg of specific energy at a specific power of 6000 and 1957 W/kg, respectively.

The Peukert Curves of the 1 and 5 Ah BOLDER cells are shown in Fig. 5. It is estimated from the Peukert

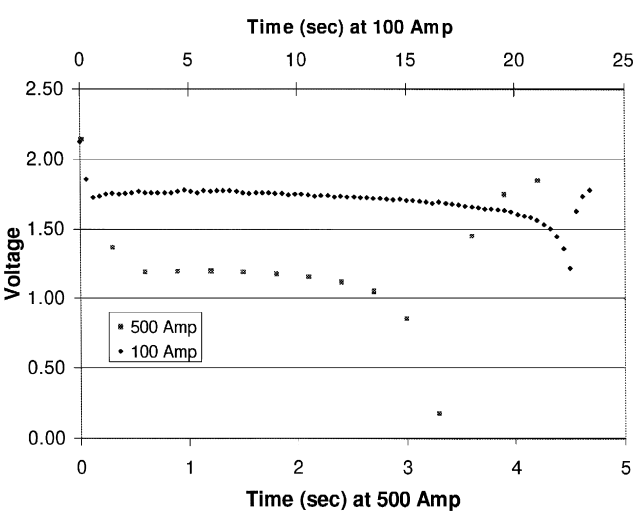

Fig. 3. Time and voltage curve at 100 A and 500 A discharge for 1 Ah TMF cell.

Table 2
Power and energy data for 1 Ah cell

	Watts (W)	Average voltage (V)	Average current (A)	Run time (s)	Specific power (W/kg)	Specific energy (Wh/kg)
Constant power discharge (W)						
86	86	1.85	47.0	60	1.049	17.5
44	44	1.90	23.2	160	0.537	23.9
24	24	1.95	12.3	300	0.293	24.4
14	14	1.97	7.1	558	0.171	26.5
Constant current discharge (A)						
500	600	1.20	500	2.8	6.997	05.4
270	364	1.35	270	6.1	4.439	7.52
200	300	1.50	200	9.1	3.659	09.2
100	175	1.75	100	25.0	2.134	14.8
100/−18°C	160	1.60	100	11.5	1.951	06.2
80	144	1.80	80	25.2	1.756	12.3
50/−18°C	86	1.72	50	26.5	1.049	07.7
1	2	2.0	1	4400	0.025	29.8

Curve, that the cells will sustain currents of up to ~1000 to 1500 A, respectively, for 0.5–1 s, which would be a specific power level of ~10,000–15,000 W/kg.

The constant current discharge performance clearly indicates that the TMF cell is a good candidate for high-power pulsed applications. The pulse power characteristics of the 1.0 Ah BOLDER cell at 100 A with an ultra-fast time response has been published earlier [10]. The important aspect of TMF cells for pulse power is their sustained delivery of high power pulses even at 80% depth of discharge and beyond.

5. Comparison with other battery technology

Rechargeable battery systems use a number of different electrochemistries, the most common of which include lead acid, nickel-metal hydride, lithium-ion and nickel-cadmium. The performance characteristics of these systems are different and have advantages in different applications. For example, lithium-ion batteries have high value and market penetration in supplying energy for laptop computers because of their ability to store a large amount of energy in a small lightweight package. This application requires very little power and is ideally suited to the characteristic of lithium-ion batteries. Lithium-ion batteries do not deliver high power, but do store and deliver higher amounts of energy than other battery eleotrochemistries. Fig. 6 shows the plot of specific power versus specific energy for different battery chemistries. The data for Fig. 6 were obtained from [12,13].

It can be seen that TMF batteries enjoy the same advantage in power delivery as lithium-ion has in energy delivery. TMF batteries deliver significantly more energy than other electrochemical systems when that energy is provided at high power rates. Fig. 6 indicates that the TMF battery is capable of six times the power delivery of other battery systems. Applications with short-duty cycles, which

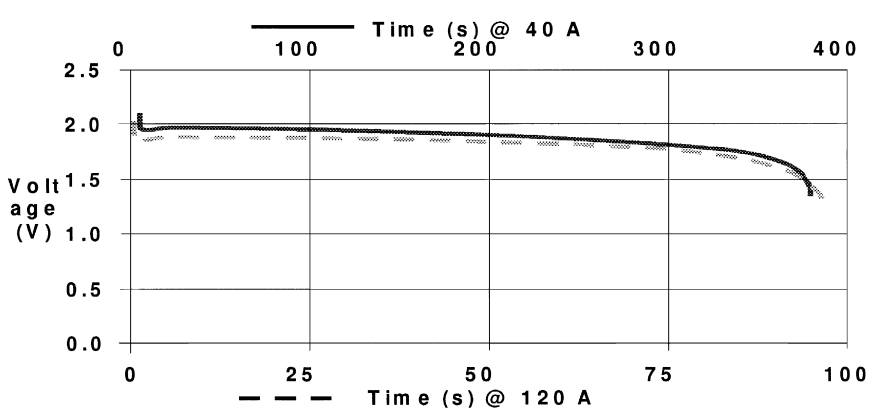

Fig. 4. Time and voltage curve at 40 A and 120 A discharge for 5 Ah TMF cell.

Table 3
Power and specific energy data for 5 Ah TMF cell

Constant current discharge (A)	Watts (W)	Average voltage (V)	Run time (s)	Specific power (W/kg)	Specific energy (Wh/kg)
1000	1600	1.60	6.0	3478	5.80
500	900	1.80	11.5	1957	6.30
200	366	1.83	51.0	796	11.30
120	224	1.87	90.0	488	12.20
40	76	1.90	370.0	165	17.00
5	10	2.00	3600.0	22	21.70
0.25	0.5	2.00	83400.0	1.1	25.20

require extreme levels of power to operate, can now be made portable; where this was not previously possible.

6. Specific applications

6.1. Jump starting auto engines

BOLDER technology has recently announced a 1.0 Ah/12 V-Engine jump-start product made from the 1 Ah/2.0 V cells. The six cells weigh around 0.5 kg and the to be weight of the unit with cable is 1.5 kg. Fig. 7 shows a picture of the jump-start product. The reports from beta testing of 70 units indicates that the product is capable of starting four to eight cylinder engines at temperatures from −20 to 50°C. Fig. 8 shows the current–time curves providing 300 A to start an engine with a single charge. The 1.0 Ah/12 V battery can start a car engine 25 times before needing another charge. Fig. 9 shows the current–time curve during the ultra-fast charge at constant voltage of 2.55 V. It is interesting to note that such a lightweight small battery is capable of supplying 300 A several times to support an engine start and can be re-charged in a few minutes. The performance characteristics clearly indicate that this unit is a good candidate for constant power and other pulse power applications.

6.2. Small aircraft engine start application

The performance results of a small aircraft start application can be found in [14,15]. The TMF Start-Stick™ product with a 1.0 Ah/12 V and 2 Ah/24 V configuration is made from 6, 12 or 24 TMF cells of 1.0 Ah/2 V. Fig. 10 shows the 12 V battery capable of delivering 600–1000 A. The Start-Stick weighs from 1.1 to 3.0 kg. The 12 V utility version of the Start-Stick started a 60 hp HKS aircraft engine 51 times before requiring recharging and was recharged in just 15 min. The StartStick is based on TMF technology and was the winner of the Stan Dzik Memorial Award at EAA AirVenture 1998.

6.3. Hybrid electric vehicle (HEV) application

Currently, there are two concepts for configuring a heat engine/battery hybrid power train. The so-called ‘dual mode’ HEV employs a relatively large battery system, in the order of 6–10 kWh at ~300–360 V, usually operated

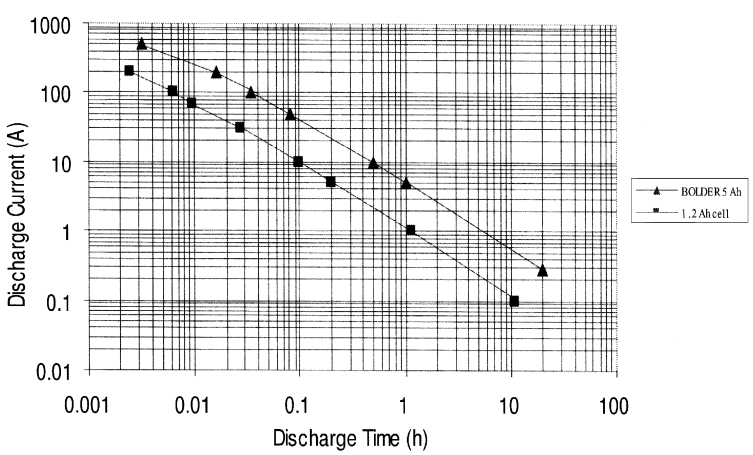

Fig. 5. Peukert curve for 1 Ah and 5 Ah TMF cell.

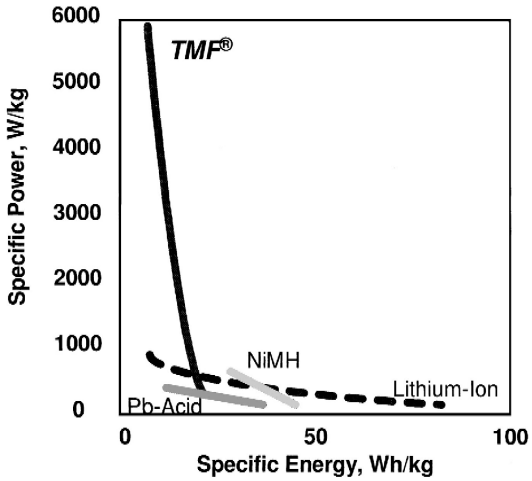

Fig. 6. Plot of specific power vs. specific energy for different battery chemistries.

in series with the heat engine. This larger battery provides a 30–50 mile 'all electric' driving range and a relatively large sink for uptake of regenerative braking energy (regen), but it has the obvious drawback of added weight and cost. The 'power assist' HEV has a much smaller battery in series or parallel with turbine or diesel heat engine. Here, the battery is at only 1–2 kWh. Still, at 300–360 V, it provides auxiliary power to the heat engine for acceleration and hill climbing and takes up regenerative braking energy as in the 'dual mode' configuration. There are various pros and cons published on the choice of series or parallel configurations, but one difference is clear. A 'dual mode' HEV battery must be relatively large in capacity and must have reasonable specific power capabilities (200–400 W/kg) while a 'power assist' HEV battery must be as small as possible while having specific power performance roughly an order of magnitude greater. It can be seen from the data given in Tables 1 and 2 that TMF technology is better suited for the 'power assist' HEV

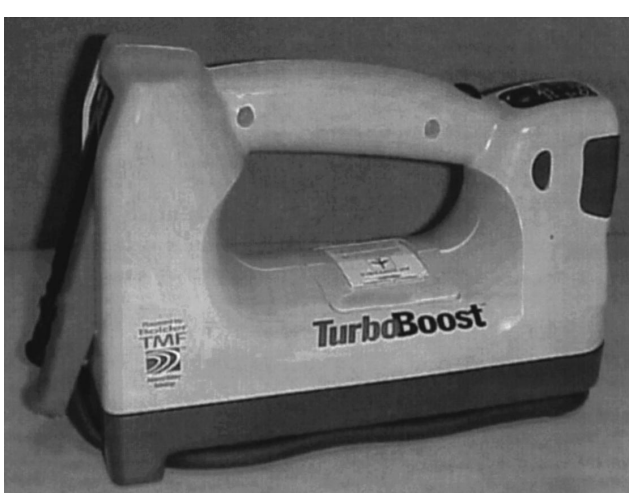

Fig. 7. Picture of 1 Ah/12 V jump-start product.

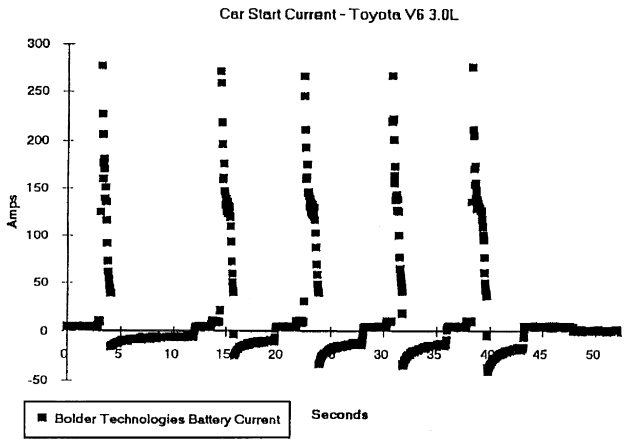

Fig. 8. Current–time curve showing supply of 300 A current during engine start.

system. The most taxing aspect of battery performance in the 'power assist' configuration is the capability of a relatively small unit to absorb large amounts of energy during regenerative braking events.

Clearly, there is more to selection of a suitable battery for an HEV than the considerations above. In a 'power assist' HEV, the battery is operated in a partial state-of-charge (PSOC), typically somewhere between 40 and 60%, and it is 'cycled' to shallow levels either side of this nominal level, as shown in Fig. 11. These power pulses are in the order of 20–30 kW for 10–20 s each and are likely to be in a random sequence.

Standard cycle tests for 'power assist' HEV batteries are in the early stages of development, and, at this time, no simulated duty cycle has been widely accepted. Power delivery and acceptance is only a part of the cycle life situation for these batteries, as a calendar life of 5–10 years is desired, and, for some portion of this duration, the battery will likely be on open circuit at some PSOC. This is a very unusual duty cycle for a VRLA product, so it is difficult to estimate cycle life values. A crude duty cycle test has been carried out at BOLDER on TMF single cells, as shown in Fig. 12. This is a preliminary test and does not address the calendar life issues. However, the cycles achieved (~43,000) are noteworthy.

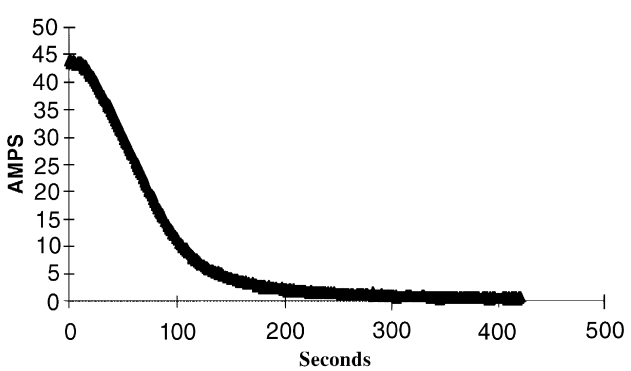

Fig. 9. Current–time curve during ultra-fast charge at constant voltage of 2.55 V.

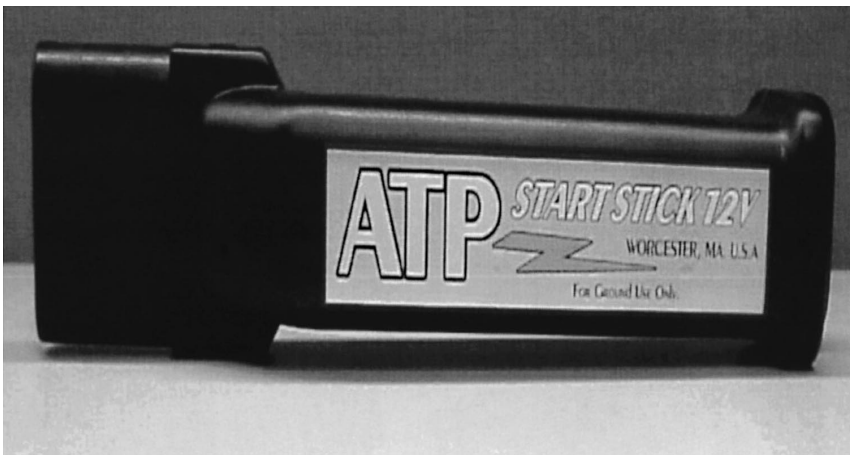

Fig. 10. Picture of 1 A/12 V Start-Stick capable of starting aircraft engine.

Vehicle operation under varying conditions is also a concern, particularly at low temperatures. As mentioned previously and demonstrated in Table 3, low-temperature operation is a strength of TMF technology. Data pertinent to HEV operation at 0, 20 and 70 F is shown in Fig. 13. It can be seen that when the battery is discharged from 100% SOC, the 20 s power levels are high and do not drop significantly in going from ambient conditions to lower temperatures. Discharges from 50% SOC show lower specific power levels as expected, but are more constant over the temperature range tested. This is another example of the superior power delivery capabilities of the TMF technology under simulated HEV usage conditions.

A further example of the power discharge performance and load leveling among the cells is shown in Fig. 14, which is a 300 A discharge of a 4×4 series/parallel matrix HEV test module developed at BOLDER. The current distribution throughout the 16-cell matrix is shown throughout the discharge. It can be seen that the current is fairly evenly distributed for about 90% of the discharge time, then the stronger cells carry increasingly more current as the weaker cells drop out. However, in the normal range of operation for an HEV battery (30–70% SOC), the current distribution is very uniform, this at a specific power level of ~ 1.7 kW/kg. As this is about the maximum value anticipated in HEV usage, it is felt that power delivery is adequate for the technology to satisfy the requirements for a 'power assist' HEV energy storage device without the voltage on load dropping below the lower limit of ~ 1.70 V/cell required by the vehicle system electronics.

The battery must also be capable of accepting large current pulses related to regenerative braking events. Here, the system electronics requires that the voltage should not

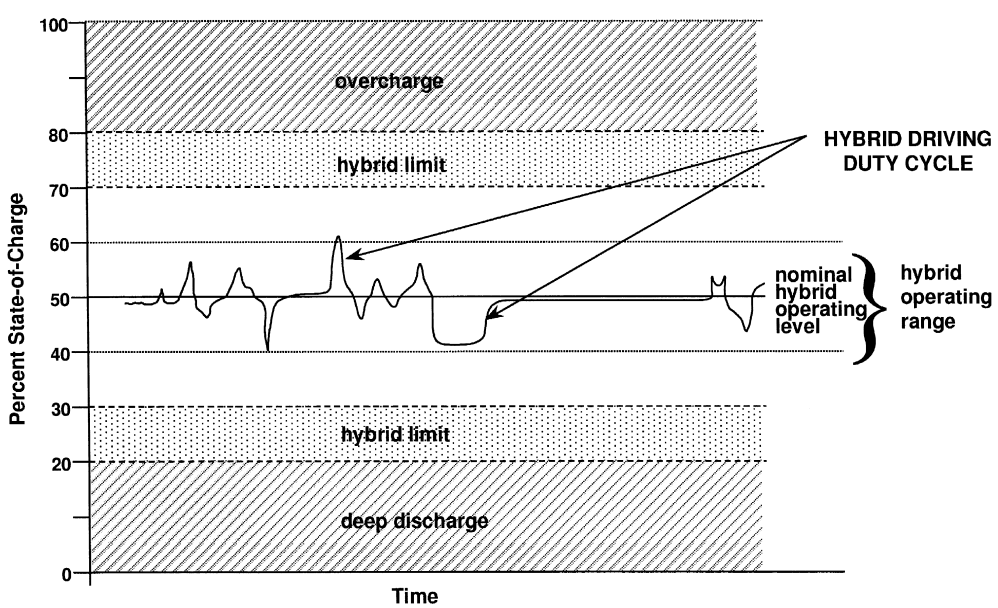

Fig. 11. State of charge considerations for HEV operation.

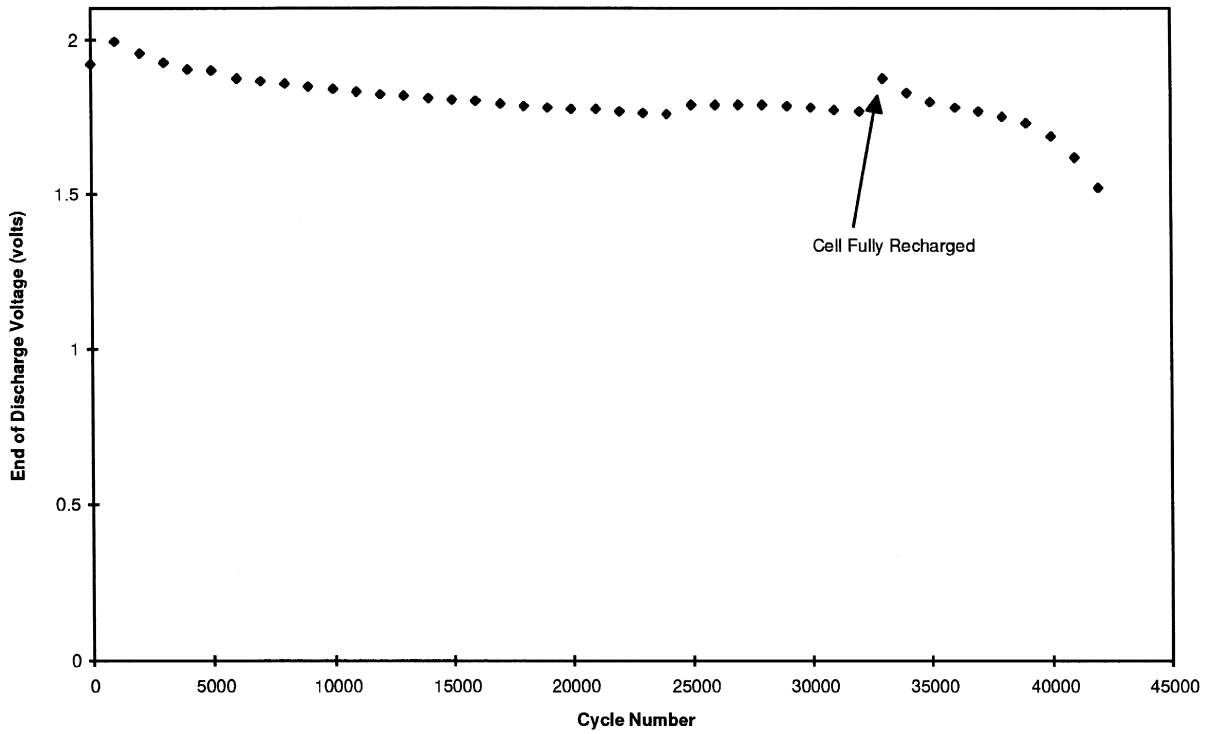

Fig. 12. Cycle graph of 1 Ah/2.0 V cell at 50% DOD for simulated hybrid duty cycle.

exceed about 2.5 V/cell at any time during the roughly 10 s charge periods. Again, the battery is operating at a nominal 40–60% SOC and a maximum charge acceptance event will entail about a 5% increase in SOC. In Table 4, end-of-charge voltages are given for such charge-acceptance events initiated at different SOC levels. It can be seen that from a 60% SOC even a 10 A charge for 20 s results in unacceptably high voltages. On the other hand, charge acceptance at a 40% SOC is excellent even at 25 A (20C rate) for 8 s. In general, it appears that the TMF technology is somewhat stronger on discharge than on charge and, thus, it will perform better if operated at a lower SOC, say 40–45%. This has the drawback of limiting the all-electric driving range somewhat, but in the 'power assist' HEV configuration use of the battery in the all-electric mode is intended to be minimal. Uptake of regen without driving the battery into heavy overcharge is a key requirement in this application, so the charge-acceptance efficiency of the battery will be a significant factor in determining the sizing in terms of Ah capacity. As mentioned, a 'power assist' battery is intended to be about 1.5 kWh, which corresponds to a 5 Ah single cell module for a 300 V battery. Sizing up from the test data shown in Table 3, such a 5 Ah cell should be able to absorb currents of up to 100 A if it is operated at a nominal 40% SOC. This should be adequate in most cases for a passenger car.

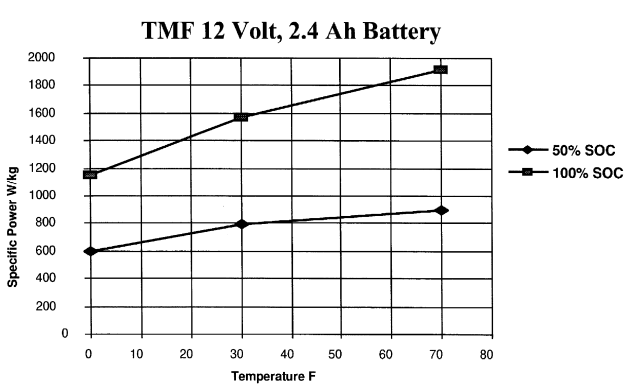

Fig. 13. Plot of temperature vs. peak power at 50 and 100% state of charge for 20 s peak power.

6.4. HEV battery design and operation

BOLDER has tested a 300 V/4.8 Ah 'power assist' battery in the Dodge Intrepid ESX diesel/battery HEV concept car; previously, a similar battery was extensively road tested in a Chrysler mule vehicle. The battery is comprised of 600 2 V/1.2 Ah single cells in a 150×4 series/parallel matrix configuration as shown in Fig. 15. This means that the four 150-cell series strings are in parallel, but then there are cross-connections between each pair of cells. The matrix approach has the advantage of isolating weak or defective cells and allowing current to flow around them so that the battery, while weakened somewhat, is still operational. However, when one of the four parallel cells 'goes out' the same currents must be handled by the remaining three cells, resulting in enhanced stress on those members. It should be stressed that this battery is by no means optimized from the standpoint of packaging or electrochemistry, but was put together with

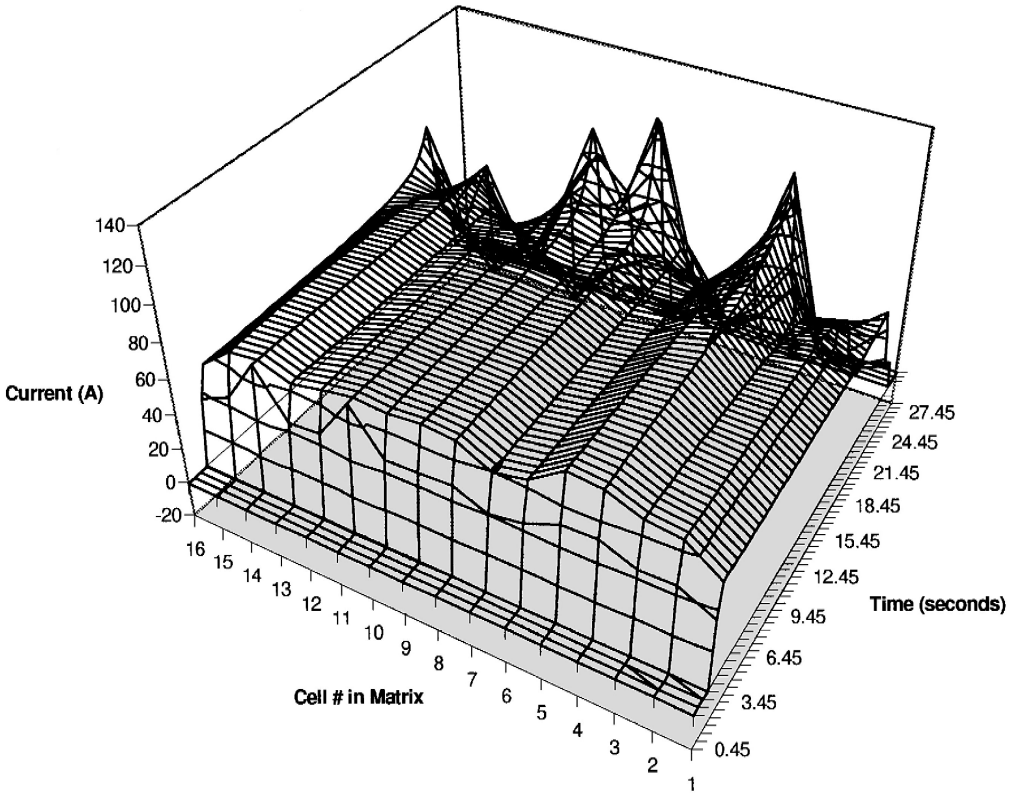

Fig. 14. Simulated HEV battery testing 8 V/4.8 Ah matrix for 1 Ah cells at 300 A discharge, showing load leveling.

BOLDER's prototype 1.0 Ah cell that was developed primarily for power tool and UPS applications.

The battery is comprised of 10 trays of 60 cells each, with said trays nesting in two five-tray stacks toward the front of the vehicle. The full battery weighs about 91 kg, of which about 49 kg are functional cells. Completely assembled, the battery is 0.635 m in length × 0.33 m in width × 0.35 m in height. The measured battery impedance, with all intercell connectors, was 61 mΩ. Because of this extremely low impedance, the battery can be operated without thermal management.

Driving tests were performed using both electric-only and HEV driving modes. Initial tests were performed limiting the total power available to the motors to 50 kW. Later, after some of the control issues had been resolved, the power limit was increased to 100 kW. Peak currents of up to 370 A were recorded from the battery. Under this magnitude of load, the battery voltage was measured at ~ 270 V at the 50% SOC level, thus providing 99.9 kW or about 1.1 kW/kg for the full battery (2.0 kW/kg for the bare cells). Acceleration to 60 mph was measured at 12.3 s for the vehicle. Charge acceptance from the alternator immediately following the accelerations was found to be excellent, with the battery accepting peak recharge currents of over 100 A at voltages below 350 V, or 2.33 V/cell (row). The charge current decreased as the battery voltage increased. Recharge was typically discontinued when the battery SOC exceeded 70%. Overall, the mule vehicle testing showed that the battery is compatible with the diesel APU and control electronics and that continuous operation at a PSOC is feasible for the TMF technology, at least in the short term.

Table 4
End of voltage for 5% recharge

DOD%	Charge current/charge time				SOC%
	10 A/20 s	15 A/13 s	20 A/10 s	25 A/8 s	
40	2.67	2.88	2.94	2.97	60
50	2.29	2.42	2.55	2.65	50
60	2.21	2.30	2.38	2.46	40

Current and future work will involve the development of a larger cell specifically designed for HEV applications — it is estimated that the capacity will be in the range of 5–7 Ah. This cell will have an electrochemical design optimized for, primarily, charge acceptance and cycle life. In connection with this, a valid cycle life duty cycle for 'power assist' HEV operation will be developed. In addition, an effective, accurate state-of-charge monitoring method will be refined (currently, a combination of open-circuit voltage and current pulse voltage drops is employed) and an overall maintenance strategy for the battery system must be developed. This maintenance algorithm will probably have more to do with determining the health and lifetime of the HEV battery system than any other factor involved to date. Therefore, it is imperative that

Fig. 15. Single tray of 300 V/4.8 Ah prototype battery used in Dodge intrepid ESX.

each battery system has a strategy that is closely tailored to the capabilities of both the vehicle and the cell modules comprising the total system.

6.5. Power quality

The increased sensitivity of modern electric and electronic equipment to power system disturbances have led to active research in the field of power quality area over the past decade. Of these disturbances, voltage sags and momentary interruptions are the most disruptive and adjustable speed drives (ASD's), which are prolific in the manufacturing industry and are among the more sensitive equipment. Voltage sag is defined as a decrease in rms voltage of between 10 and 90% of nominal voltage, for periods from a half cycle up to a minute long, whereas a momentary interruption is a decrease in rms voltage $> 90\%$ [16]. The detailed survey of voltage sags and their magnitude is described by Annabelle and Spee [17] along with the power requirements to rectify the problem. Although

Table 5
Comparison of energy storage systems for ASD ride-through

System qualities	Units	Low speed flywheel	Ultra-capacitors	TMF batteries
Maximum constant power	kW	240	100	100
Maximum duration discharge	s	13.5	5.0	15.0
Nominal output voltage	V	550	800	585
Output voltage regulation during discharge	%	1	< 2	< 2
Initial storage energy	MJ	4.25	4.80	5.90
Energy delivered to ASD (% of stored energy)	%	76	11	25
Standby losses (% of rated output power)	%	1.0	0.50	0.50
Discharge losses (% of rated output power)	%	7.0	96.0	12.0
Weight	kg	1275	375	270
Volume	m^3	1.90	1.10	0.60
Footprint	m^2	1.0	1.0	0.50
Specific power	W/kg	188	267	370
Power density	kW/m^3	126	94	173
Response Time	ms	< 4.0	< 4.0	< 4.0
Minimum recharge time	min	15–20	20.0	3–5.0
Expected life	Years	20	10–12	5–10 (new design)
Operating temperature	C	$-20/40$	0/40	$-20/40$
Maintenance intervals	Months	3	60	36–60

several techniques and technologies can be used for reliable operation of ASD's, this section addresses the use of an energy storage system which includes flywheel, ultra-capacitors and batteries, based on the criteria specifically aimed at ASD ride-through.

Flywheel energy storage systems convert electrical energy to kinetic energy through an electrical motor, increasing the rotational speed of a flywheel coupled to the rotor. During discharge, kinetic energy is converted to electrical energy through a generator. Instead of using a separate motor and generator, it is also possible to use the same machine as generator and motor, along with a bi-directional converter interface. For ASD ride-through, a dc output voltage is required in order to interface the energy storage system to the bus. Either a dc generator or an ac generator with a rectifier can be used to achieve this.

Ultra-capacitors store electrical energy by accumulating and separating unlike charges. Different material combinations are under development, e.g., a carbon composite electrode using an organic electrolyte and carbon/metal fiber composite electrode with aqueous electrolyte. Because the square of the capacitor voltage is proportional to the energy stored, the voltage drops as the capacitor discharges, necessitating a dc–dc converter interface to the dc bus to regulate the bus voltage. The capacitor output current increases as the capacitor discharges, therefore, a trade-off exists between the current rating of the dc–dc converter and the percentage of stored energy deliverable to the drive.

Batteries store and deliver electrical energy through reversible chemical reactions and many different kinds of batteries have been developed, e.g. lead acid, nickel-cadmium, nickel-metal hydride and lithium ion. Lead acid batteries have traditionally been used for uninterrupted power supply (UPS) application, currently holding two-thirds of the world market in UPS [18].

The TMF batteries manufactured by BOLDER Technologies Corporation on a commercial scale hold great promise for ride-through applications. Their design and configuration allows batteries with low internal resistance, high discharge rates and flat voltage profiles at very high discharge rates, thereby providing very high power densities.

The comparison of energy storage systems for ASD ride-through is shown in Table 4. The performance parameters of the TMF battery are provided only for a 1 Ah cell.

It is important to note that the characteristics listed in Table 3 are for integrated systems, not only the energy components. The specific details of this comparison are published by Annabelle and Spee [16].

The data in Table 5 clearly suggest that TMF lead acid battery performance is comparable with or better than all other technologies listed. The TMF battery uses lead as a primary raw material, which is the cheapest possible material to build energy storage devices.

7. Summary

TMF technology extends existing VRLA state-of-the art to a new level of performance which is capable of delivering high power not delivered by any other battery or battery chemistry. The superior power characteristics are achieved through the implementation of a design that features ultra-thin plates, very small plate spacing and a current collection/delivery path that can sustain high current levels. The batteries with TMF technology cells can be used as engine start, turbine start, HEV or any high pulse power application.

Acknowledgements

The authors wish to thank Teri A. Farmer and Karen Egger, Executive Assistant at BOLDER Technologies Corporation for their assistance in editing and preparation of this manuscript.

References

[1] T.J. Juergens, U.S. Patent No. 5,045,085 (1991).
[2] T.J. Juergens, U.S. Patent No. 5,047,300 (1991).
[3] T.J. Juergens, U.S. Patent No. 5,198,313 (1993).
[4] T.J. Juergens, M. Ruderman, R. Brodd, Proceedings of the 9th Annual Battery Conference Applications and Advances, 1994, pp. 45–48.
[5] R.F. Nelson, David M. Wisdom, J. Power Sources 33 (1991) 165–185.
[6] R.F. Nelson, 11th Annual Battery Conference on Applications and Advances, IEEE, Piscataway, NJ, 1996, p. 173.
[7] R.F. Nelson, J. Keating, R. Rinehart, Proceedings of the Power 96 Conference, Santa Clara, CA, October, 1996.
[8] R.C. Bhardwaj, Proceedings of the 14th International Seminar on Primary and Secondary Batteries, Fort Lauderdale, FL, 10–13 March, 1997.
[9] R.C. Bhardwaj, R. Rinehart, J. Keating, Proceedings of the 13th Annual Battery Conference on Applications and Advances, California State University, Long Beach, CA, 13–16 January, 1998.
[10] R.C. Bhardwaj, L. Gillman, Proceedings of the 15th International Seminar on Primary and Secondary Batteries, Fort Lauderdale, FL, 2–5 March, 1998.
[11] R.C. Bhardwaj, J. Power Sources 3320 (1999) 30.
[12] Franz J. Kruger, Proceedings of the 15th International Seminar and Exhibit on Primary and Secondary Batteries, 1998.
[13] BOLDER Technologies Corporation, TMF database on product testing of Companies Production cells, 1998.
[14] Fred Roberts, Sports Pilot Ultralights, 1998.
[15] Industry Week, 1998.
[16] D.D. Sabin, A. Sundaram, IEEE Spectrum, 1996, pp. 34–41.
[17] Annabelle V. Zyl, Rene Spee, Proceedings of the 33rd Annual Meeting of Industry Application Society of IEEE, St. Louis, MO, October, 1998.
[18] D. Linden, Handbook of Batteries, 2nd Edition, McGraw Hill, New York, 1995.